

Separation delay on thick airfoil using multiple synthetic jets

Davide Lasagna¹, Salvatore Donelli², Fabrizio De Gregorio², Matteo Orazi¹, Gaetano Iuso¹

¹*Department of Mechanical and Aerospace Engineering, Politecnico di Torino, Italy*

E-mail: gaetano.iuso@polito.it

²*C.I.R.A. spa*

Capua (Caserta), Italy

E-mail: r.donelli@cira.it

Keywords: Flow control, synthetic jets, separation delay.

SUMMARY. High momentum 2D synthetic jet actuators are tested experimentally focusing the investigation on the separation delay over the airfoil NACA 0024 at high angles of attack. Four slots are present on the suction side of the airfoil. The number of slots in the downstream direction, the position and the width of the active slots and the forcing frequency were varied to investigate on their effects produced. Pressure measurements and wake analysis were performed at Reynolds number equal to 10^6 . A weak influence was observed at low and medium incidences on the lift and drag curves. Considerable increments of the lift coefficient also associated with drag reductions were obtained at high angles of attack according to the values of the forcing frequency and the slots configuration. The influence of the slot width does not highlight great differences on the lift and drag curves. The upstream location of the slots is more effective to delay separation compared with further downstream positioning. Two consecutive active slots were effective as a single one at the same frequency while the estimated comparison at constant momentum could allow better performances. The tests were carried out operating with forcing frequencies near the resonance conditions of the system synthetic jet- cavity-pneumatic line.

1 INTRODUCTION

The separation control is a widely investigated topic due the large influence of the separated flow on the aerodynamic performance of both streamlined and bluff bodies. Steady and unsteady forcing are extensively used to control flow separation. Seifert et al. [1] have demonstrated that much less power is required to produce equivalent increases in the lift coefficient for oscillatory control rather than for steady blowing techniques. Results related to the unsteady forcing show that the optimum reduced frequencies $F^+ = f x_{te}/V_\infty$ for separation control are in the range $0.3 < F^+ < 4$ for most cases. Many papers have been devoted to investigate on the potentiality of synthetic jets as flow separation control device. Glezer and Amitay [2] gave an exhaustive review on the basic characteristics of synthetic jets and on their applications for the flow control around streamlined and bluff bodies. The interesting aspects of such forcing rely on the possibility to tune the two forcing parameters, oscillation frequency and amplitude, in order to generate the most appropriate length and time scales for the given flow to be controlled.

Application of synthetic jets to control the laminar separation under the effects of adverse pressure gradient on a flat plate have been proposed by Guang Hong [3]. The author used specific forcing frequencies to trigger T-S instability in order to accelerate the viscous transition. The

separation delay is vital near stall conditions where aerodynamic performance deteriorate rapidly. Higher lift and increased stall incidence, possibly associated to low drag, are required to have an efficient flow control technique. The use of synthetic jets for stall delay has been proposed by Donovan et al., [4] ; Seifert et al., [5] and by Duvigneau and Visonneau [6].

The synthetic jet injection point can be placed in the region of the leading edge to generate virtual shaping as proposed by Mittal et al. [7] and by Orazi et al. [8]. Tuck and Soria [9] also used synthetic jet mounted on the leading edge of a NACA 0015 airfoil to actively control flow separation and enhance lift. Experiments were conducted at low Reynolds number and evidenced that the largest lift increase was obtained for a non-dimensional frequency of 1.3 to which corresponded a momentum coefficient equal to 0.0014. Amitay et al. [10] achieved an increase of the stall incidence from 5° to $17,5^\circ$ on a unconventional airfoil. The momentum coefficient required to reattach the separated flow decreased as the actuator was placed closer to the separation point. Further downstream locations of the synthetic jet injection are also very effective to delay separation.

Wilson et al. [11] experimentally investigated the effects of a 2D synthetic jet positioned at $x/c=0.30$ and $x/c=0.65$ on a thick NACA 0036 airfoil at a Reynolds number equal to 10^6 . Forcing frequencies up to 120Hz were tested, giving a maximum momentum coefficient equal to 0.0086. Hot wire measurements in the wake of the airfoil showed a reduced portion of separated flow in the controlled conditions and brought the high Reynolds shear stress layer closer the airfoil surface.

Holman et al. [12] experimentally studied the interaction of adjacent synthetic jets with the cross flow developing on a NACA 0025 airfoil at an angle of attack of 12° and a Reynolds number equal to 10^5 . The authors used piezoelectric actuators varying the relative phasing and the oscillation frequency and amplitude to control the flow separation. The authors observed that the jet formation was not a necessary condition to achieve an effective control. Moreover, also the relative phasing of the jets did not appear to play a significant role in the separation delay.

The main motivation of the present work is primarily related to the lack of results inherent to the use of very high momentum injection to control the flow separation on airfoils at high angles of attack and high Reynolds number. Another goal related to the applicability of the flow control actuators was the development of compact, low weight, low power consumption and reliable system for long duration employments.

2 EXPERIMENTAL SETUP AND MEASUREMENTS TECHNIQUES

The experiments were arranged in the wind tunnel of the Mechanical and Aerospace Department of the Politecnico di Torino. The circular test section is characterized by diameter and length equal to 3m and 5m respectively. The airfoil chord and spanwise length of the model were respectively equal to 500mm and 1200mm. The model was realized in aluminium and manufactured by numerical control machining. Two large rectangular end plates were mounted at the extreme parts of the model extending from two chords upstream the leading edge up to 3 chords downstream the trailing edge. Static pressure taps were distributed on the model for a total of 128, most of which positioned in the middle section while the others were located on a parallel section at 200mm from one endplate. The static pressure taps on the model surface were connected to two ZOC33 Scanivalve pressure transducers, each of them allowing to measure up to 64 channels. The full scale is equal to ± 10 inches of H_2O for 56 channels pressure inputs and ± 20 H_2O inches for 8 channels pressure inputs. The latter have been connected to the pressure taps located where the maximum suction peak was expected. The transducers have an accuracy of 0.15% of the full scale. The ZOC33 modules have been located inside the model and an Ethernet

cable was used for the data transmission to a personal computer.

The airfoil was mounted vertically on two round tables flush with the two end plates. At the two round plates two cylindrical supports were fixed, the lower one was anchored to a remotely controlled turning table, which allowed to finely adjust the model's angle of attack. The upper support was free to run inside a bearing that allowed only minimum angular misalignments over the 3 meters of length. The suction side of the wing model presented a box covered by a rectangular plate having four equal rectangular slots aligned with the spanwise direction of the model. The synthetic jets emerged from the slots perpendicularly to the airfoil surface. By varying the cover plates was possible to change the slots width. In table 1 the streamwise positions and width for slot pertaining to each panel are reported.

| Slot | Position x/c | Width h [mm] | | | |
|------|----------------|----------------|---|-----|---|
| s 1 | 0.449 | 0.5 | 1 | 1.5 | 2 |
| s 2 | 0.497 | 0.5 | 1 | 1.5 | 2 |
| s 3 | 0.545 | 0.5 | 1 | 1.5 | 2 |
| s 4 | 0.594 | 0.5 | 1 | 1.5 | 2 |

Table 1 Locations and width of the slots for each cover panel.

For each cover plate different configurations were allowed by simply closing with tape some of the slots. In this way it was possible to test the effects of the distance between the slots, the number of the active slots and their width. For each configuration the effects of the forcing frequency was investigated. In figure 1 the pictures of the wing interior (a), of the cover plate (b) and of the synthetic jet actuator (c) are reported.

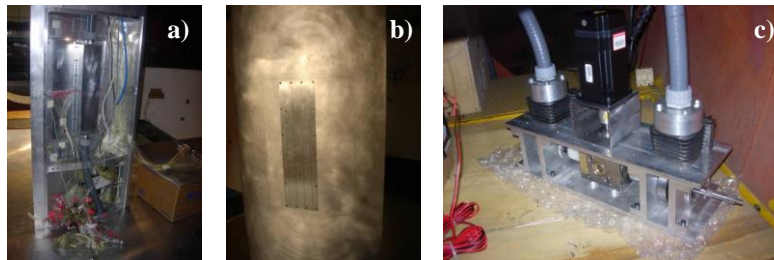


Figure 1. a) Synthetic jets module in wing b) Suction side with the multiple synthetic jet slots
c) Synthetic jets actuators

The synthetic jets plates covered a rectangular plenum inside the airfoil which was fed through two pneumatic tubes ($d_{\text{internal}} = 1''$) mounted on the sides of the plenum. The other extreme ends of the tubes were connected to the synthetic jets actuators located outside the wind tunnel. The total length of the pneumatic tubes was equal to 8.1m.

The synthetic jets actuator was designed and built using the crank-rod system from two motorcycle engines which were characterized by bore and stroke equal to 39 and 41.8 mm respectively. The two oscillating systems were driven by a remotely controlled brushless electrical motor. Two aluminium cylinders were used as interfaces between the output of the engines and the input of the pneumatic tubes.

The wake analysis was performed to evaluate the airfoil drag. A wake rake having 96 total

pressure probes and 5 static probes was positioned downstream the airfoil at a distance equal to 3 chords from the trailing edge. The total and static pressure measurements in the wake were performed with three DSA3217 Scanivalve pressure transducers having 16 input channels each. The full scale is equal to ± 10 inches of H₂O and the accuracy is equal to 0.2% F.S. Also in this case the data transmission between the Scanivalve transducers and the pc was implemented by means of the TCP/IP protocol. The arrangement of the wake rake behind the model is shown in figure 2a while the final setup in the test section is shown in figure 2b.

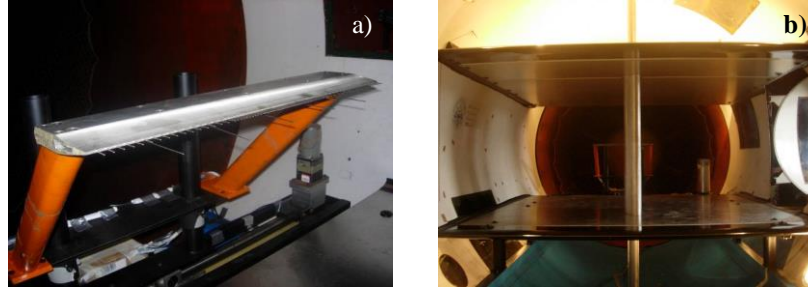


Figure 2. a) Wake rake b) Test section configuration

3 DATA REDUCTION

Lift coefficient was evaluated by integrating the pressure distributions around the model. The drag coefficient was estimated by means of the momentum balance over a control volume using the measured total pressure distributions and the static pressure values from the wake rake measurements. Jones' formula, as reported by Schlichting, [13] was used in the computations of the drag coefficient.

$$C_D = 2 \int \sqrt{\frac{p_{t2} - p_2}{q_\infty}} \left(1 - \sqrt{\frac{p_{t2} - p_\infty}{q_\infty}} \right) d\left(\frac{y}{c}\right)$$

Here the pedicels 2 and ∞ refer to measurement section and free stream conditions, respectively; c is the model's chord; p_t is the total pressure in the wake, p the static pressure and q_∞ the free stream dynamic pressure. Wind tunnel wall corrections, lift interference, solid and wake blockage, were taken into account as described in reference Agard [14]. The corrections were less than 5% over all the range of incidences tested. The accuracy of the aerodynamic coefficients was also evaluated as outlined in Agard [15].

4 RESULTS

The investigation was carried at a Reynolds number equal to 10^6 based on the airfoil chord and on the upstream velocity equal to $V_\infty=30$ m/s. Three different cover plates were used with slots width equal to $h=0.5$ mm, $h=1$ mm and $h=2$ mm. A preliminary investigation was devoted to the synthetic jet characterization in still air using the synthetic jet module outside the model.

4.1 Synthetic jet characterization

The power and the characteristic time of a synthetic jet are identified by two forcing parameters, namely the momentum coefficient C_μ and the non-dimensional frequency F^+ defined

respectively as follow :

$$C_{\mu} = \frac{h V_{sj}^2}{c V_{\infty}^2} \quad F^{+} = \frac{f c}{V_{\infty}}$$

The axial jet velocity V_{sj} was measured using a miniaturized pressure probe positioned at $y=5h$ from the exit section to avoid reversed flow. Velocity distributions were measured along the span and width of the slot. The characterization was carried out over a wide range of frequencies and for slot widths of $h=1\text{mm}$ and $h=2\text{mm}$. In figure 3 the velocity on the jet axis as a function of the frequency of oscillation is reported. As can be observed for both widths a resonant behaviour is highlighted for which the jet velocity rises considerably. Four resonance frequencies were revealed for each slot width evidencing increasing velocity peaks with the frequency. The maximum velocity was of about 37 m/s for the thinner slot at the frequency around 70Hz. A weak shifting of the resonant frequencies was present for the two slot widths, the thinner one showed slightly higher resonance frequencies.

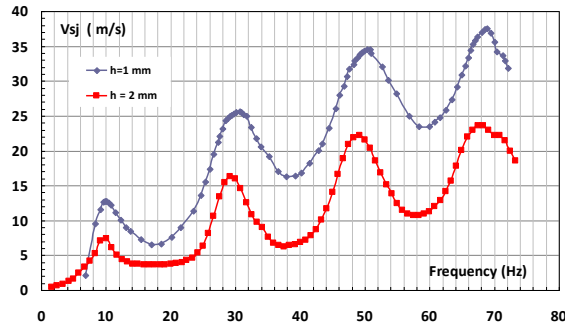


Figure 3. Velocity distributions at the slot exit varying the frequency. $y = 5h$

The investigation was therefore performed working at frequencies equal to the mean between those of the two slots widths for the three highest resonance frequencies. For the free stream velocity corresponding to the Reynolds number equal to 10^6 the values of the non dimensional forcing parameters C_{μ} and F^{+} are reported in table 2. For $h=0.5\text{mm}$ the jet velocities were extrapolated at the three frequencies.

| f (Hz) | $C_{\mu} \cdot 10^{-3}$ | | | F^{+} |
|--------|-------------------------|-------|-------|---------|
| | h=0.5mm | h=1mm | h=2mm | |
| 26.7 | 1.983 | 1.502 | 1.138 | 0.445 |
| 50 | 3.294 | 2.722 | 2.250 | 0.833 |
| 68.3 | 3.615 | 3.042 | 2.560 | 1.138 |

Table 2. Forcing parameters corresponding to $V_{\infty}=30\text{m/s}$.

4.2 Effects of the forcing on the Lift and Drag curves

Most of the results presented are related to the range of incidences corresponding to the high angle of attack. In figure 4 the lift and drag curves are displayed in the case of slot 1 and width $h=0.5\text{mm}$. In the same figure the curves corresponding to the baseline case are reported.

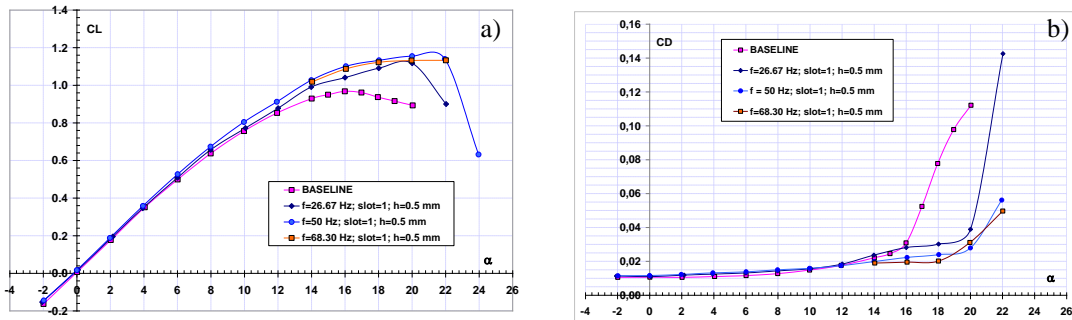


Figure 4 a) Lift curves b) Drag curves. Effects of the forcing frequency. Slot 1 ; $h=0.5\text{mm}$.

As can be seen both curves are slightly affected by the forcing frequency in the range of low medium angle of incidences. Only small beneficial effects are visible through lift increments. At the same time weak increasing of drag are observable. The most significant influences are evident at high incidences ($\alpha > 12^\circ$). In particular the maximum lift and the stall incidence both raise with the forcing frequency. In the case of $f=68.3\text{Hz}$ an increment of maximum lift around 20% is highlighted with respect to the baseline while the stall incidence moves from $\alpha=16^\circ$ for the baseline to $\alpha=22^\circ$ in the forced case. Moreover it also appears that as the frequency increases a drastic drop of the lift coefficient takes place. At high incidence as the forcing frequency increases an extension of the range of angles of attack characterised by low drag was observed. For $\alpha=20^\circ$ and for $f=68.3\text{Hz}$ a drag reduction of the order of 70% is obtained. The results of figure 4 are the evidence of the flow separation delay operated by the interaction between the synthetic jet and the cross-flow. The high mixing in the region of incipient flow separation promoted by the synthetic jets gives rises to momentum transfer directed in the wall region that energizes the near wall flow and consequently moves more downstream the separation point.

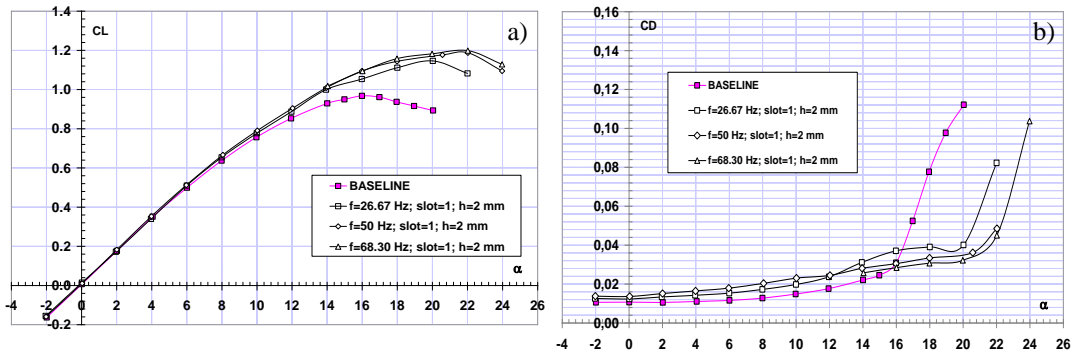


Figure 5 a) Lift curves b) Drag curves. Effects of the forcing frequency. Slot 1 ; $h=2\text{mm}$

The results shown in figure 5 differ from the previous ones by the effect of the slots width which is now equal to $h=2\text{mm}$. The lift and the drag curves behave in a similar fashion to that corresponding to $h=0.5\text{mm}$ showed in figure 4. A slightly higher value of the maximum lift coefficient is now present with respect to the baseline and a more flat stall is evident. The drag

curves remain approximately the same with exception of the lesser rising of the curves for $f=50\text{Hz}$ and $f=68.3\text{Hz}$ at the extreme incidences.

The effects of the synthetic jet slot positioning are presented in figure 6a and 6b, keeping the forcing frequency and the slot width constant and equal to 50Hz and $h=2\text{mm}$ respectively. As can be seen all the slot locations are effective in increasing the lift and reducing the drag at high angles of attack but the best performing position is the most upstream one, namely $x/c=0.449$. For $\alpha=20^\circ$ while the slot locations $s1$, $s2$ and $s3$ are still effective at maintaining the flow attached, the slot location $s4$ shows the first signs of massive flow separation as can be seen by the decrease in lift and the fast drag increase. These results are in line with those of the literature and confirm the effectiveness of the momentum injection when its location is around the point of incipient flow separation. This because a much anticipated injection with respect to the developing separation could promote the separation itself. On the other hand, injecting in the separated flow would result in a loss of effectiveness of interaction of the synthetic jet with the external flow.

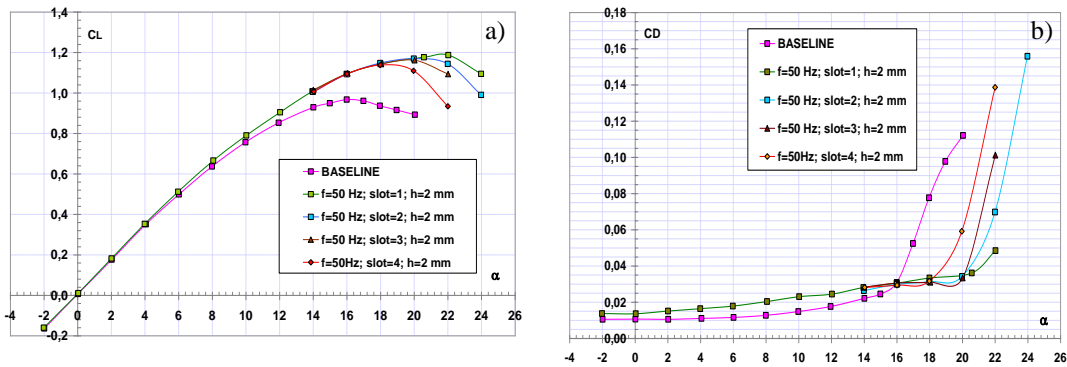


Figure 6 a) Lift curves b) Drag curves. Effects of the slot positioning. $f=50\text{Hz}$; $h=2\text{mm}$

The pressure coefficient distributions around the airfoil and the velocity distributions in the wake, made dimensionless by the upstream velocity ($V_\infty=30\text{m/s}$), are presented in figure 7a and in figure 7b respectively. The slot width and the forcing frequency are fixed and equal to $h=2\text{mm}$ and $f=50\text{Hz}$ while the angle of attack is $\alpha=20^\circ$. The effects of the active slot $s1$ and $s4$ are examined.

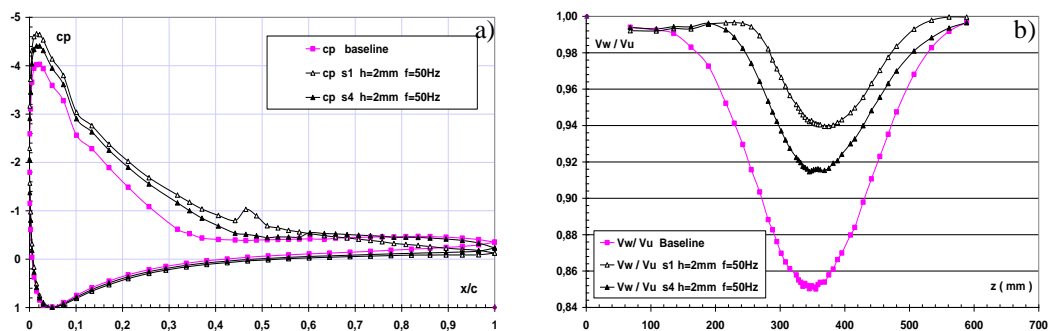


Figure 7 a) Pressure distributions b) Wake velocity distributions.
Effect of the slot location. $\alpha=20^\circ$; $f=50\text{Hz}$; $h=2\text{mm}$; $(x/c)_{s1}=0.449$; $(x/c)_{s4}=0.594$.

For the case of natural flow the separation takes place at $x/c \approx 0.4$ as evidenced by the pressure distribution on the suction side. A massive flow separation is present as highlighted by the large wake characterized by low momentum showed in figure 7b. When slot 4 is active the flow is attached up to around $x/c \approx 0.5$ while in the case of the slot 1, the flow separates approximately at the trailing edge of the airfoil, as evidenced by the continuous pressure recovery up to $x/c \approx 1$ on the suction side. Furthermore when s1 was active, a region of higher suction around the injection point is present with respect to its surrounding. This behavior is completely absent in the case of s4 injection. Interestingly, whichever is the active slot, the pressure distributions highlight considerable modifications upstream the jet injection up the suction peak. Also, the degree of the upstream pressure modification depends on the active slot. Downstream the jet injection the pressure distributions appear less influenced with respect to corresponding upstream ones.

The flow separation delay shows its characteristic also in the wake velocity distributions reported in figure 7b. In fact, with respect to the baseline, in the forced cases the wake velocity distributions are representative of less dissipative conditions that means much lower drag especially when the injection is located more upstream. In figure 8 the lift and drag curves are displayed describing the effects of a multiple injection s1+s2, for two frequencies $f=26.67\text{Hz}$ and $f=50\text{Hz}$. The slot width considered was the thinner one $h=0.5\text{mm}$. For comparison, on the same figures the baseline curves are also shown together with two curves related to the single slot s1 and s4 corresponding to the same forcing frequency.

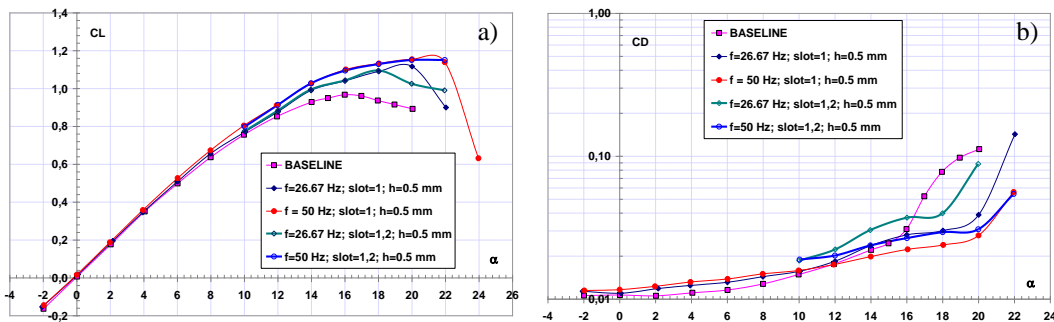


Figure 8 a) Lift curves b) Drag curves. Multiple injection : s1 + s2. $h=0.5\text{mm}$.

It can be observed that in general the multiple injection does not seem to affect the lift curves if the same forcing frequency to the single injection is applied. Moreover the multiple injection determines lower beneficial effects on drag with respect to the single injection cases. This effect appears more evident in the case of the lower frequency at high incidences for which the drag reduction benefit is decreased.

Nevertheless it has to be pointed out that a simple comparison at fixed frequency between single and multiple injection is not rigorous. Others effects should be considered for a more critical analysis such as the actual momentum injected by the single slot and by the combination of two of slots. Also the pressure drop for the different slot configuration has to be taken into account.

A more suitable comparison is done considering the same momentum injected from the single slot and the double slot. From this point of view, in order to perform a comparison at an approximately constant momentum coefficient, it would be more appropriate to take the double injection at $f=50\text{Hz}$ and the single injection at $f=26.67\text{Hz}$ cases. Given this considerations better performances could be achieved in the case of multiple injection.

Another assessment with respect to the comparison between the multiple and the single slot injection at constant momentum, can be made keeping constant the forcing frequency and also the total jet exit section. The results, not reported in the paper, show a not significant influence on the lift curves while lower drag are evidenced in the case of double slot configuration.

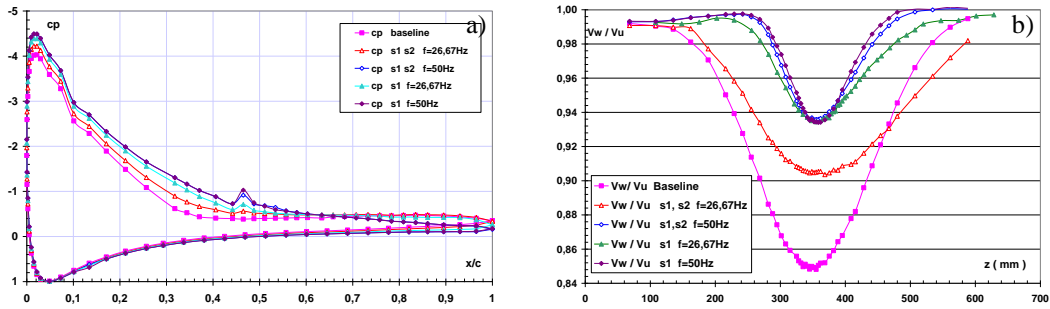


Figure 9 a) Pressure distribution around the airfoil b) Velocity distribution in the wake.
Effects of combination s1 + s2. $\alpha=20^\circ$ $h=0.5\text{mm}$

Pressure distributions around the airfoil and the velocity distributions in the wake are displayed in figure 9 for incidence $\alpha=20^\circ$ corresponding to the same cases reported in figure 8. As can be seen from figure 9a, flow separation takes place on the baseline configuration at around $x/c=0.4$ also evidenced in figure 9b from the large and very low momentum wake. The effect of the injection determines a delay of the flow detachment leading to a complete reattachment up to the trailing edge for the case forced at $f=50\text{Hz}$ and with a single slot, as also showed before. This effect is evident on the wake velocity profiles which are characterized by a considerably lower momentum deficit. For this incidence the forcing that gives rise to the poorest improvement with respect to the baseline is that related to $f=26.67\text{Hz}$ and double slot as displayed from both diagrams of figure 9a and figure 9b. The best performance enhancements have been observed for the case corresponding to $f=50\text{Hz}$ and single active slot.

5 CONCLUSIONS

An experimental investigation has been carried out to study the effects of the interaction between nearly 2D synthetic jets and an airstream on the airfoil NACA 0024. The synthetic jets were generated by a mechanical actuator suitable for high momentum injection. The effects of the forcing frequency and of different slots configurations were tested combining several widths, multiple injection and different slot locations in the streamwise direction. The forcing frequency was beneficial essentially in the range of mid-high incidences highlighting higher lift coefficient and very low drag with respect to the baseline. At the maximum frequency ($f=68.3\text{Hz}$) the $C_{L\text{max}}$ raised by 20% while the stall incidence increased from 16° to 22° . Also the slot width evidenced a valuable effect, larger slot width generated slightly higher lift with respect to those pertaining to the smaller one and also evidenced a more flat stall. The effects of the injection position revealed that the most performing interaction was obtained when the active slot was at the most upstream location $x/c = 0.449$. Much greater benefits were obtained in terms of drag reduction at high angle of attack. For $\alpha \approx 20^\circ$ the amount of drag reduction at the maximum frequency was of the order of 70%. The results on the multiple injection investigation showed that for the same frequency and

width, the added slot does not produce appreciable benefits with respect to the single injection for what concerns the lift curves. On the other hand the double slot generates higher drag with respect to the single injection. Considering a comparison at constant momentum injected a possible better performance of the double slot injection can be obtained. The pressure distributions are considerably modified from the jet injection point up to the suction peak. Downstream the injection a continuously pressure recovery up to the trailing edge region was experienced in the cases of effective forcing highlighting flow separation delay. Finally wake analysis gives evidence of lower momentum deficits in forced conditions.

References

- [1] Seifert A., Darabi A., and Wygnanski, I., "Delay of Airfoil Stall by Periodic Excitation", *Journal of Aircraft*, Vol. 33, No. 4, 1996, 691–698.
- [2] Glezer A. and Amitay M. "Synthetic jets", *Annual Review of Fluid Mechanics*, Vol. 34, 503–529, January 2002.
- [3] Guang Hong "Effectiveness of micro synthetic jet actuator enhanced by flow instability on controlling laminar separation caused by adverse pressure gradient", *Sensors and Actuators A: Physical*, Vol.132, Issue 2, pp.607-615, 2006
- [4] Donovan J.F., Kral L.D., Cary A.W., "Active flow control applied to an airfoil" 36th AIAA Aerospace Sciences Meeting and Exhibit, 1998, 10.2514/6.1998-210 (1998)
- [5] Seifert A., Darabi A., and Wygnanski, I., "Delay of Airfoil Stall by Periodic Excitation", *Journal of Aircraft*, Vol. 33, No. 4, 1996, 691–698.
- [6] Duvigneau R., Visonneau M., "Simulation and optimization of stall control for an airfoil with a synthetic jet", *Aerospace Science and Technology* 10 (2006), 279–287.
- [7] Mittal R., Rampunggoon P., "On the Virtual Aeroshaping Effect of Synthetic Jets", *Phys. Fluids*, Vol. 14, No. 4, April 2002, 1533–1536.
- [8] Orazi M., Lasagna D., Iuso G., "Virtual Shaping on NACA 0015 by Means of a High Momentum Coefficient Synthetic Jet" *International Journal of Flow Control*, Vol.3, N.4, Dec 2011.
- [9] Tuck A. and Soria J., "Active Flow Control over a NACA 0015 Airfoil using a ZNMF Jet" 15 th Australasian Fluid Mechanics Conference, Australia 13-17 December 2004
- [10] Amitay M., Smith B. L., Glezer A., "Aerodynamic Flow Control Using Synthetic Jet Technology", *AIAA Paper* 98–0208, Jan. 1998.
- [11] Wilson J.S., Preston B.M., Tung C., Tso J., "Turbulence Measurements of a Two-Dimensional NACA 0036 Airfoil with Synthetic Jet Flow Control", 24th AIAA Applied Aerodynamics Conference, 2006, 10.2514/6.2006-3157
- [12] Holman, R., Gallas, Q., Carroll, B. and Cattafesta, L. "Interaction of adjacent synthetic jets in an airfoil separation control application" in *Proc. 33rd AIAA Fluid Dynamics Conference and Exhibit*, Orlando, Florida, June 23-26, 2003, (AIAA 2003-3709).
- [13] Schlichting, H., *Boundary-Layer Theory* McGraw-Hill Series in Mechanical Engineering (1968)
- [14] Agard (1998) Quality assessment for wind tunnel testing. NATO Research and Technology Organisation, Neuilly-sur-Seine
- [15] Agard (1994) Wind tunnel wall corrections. NATO Research and Technology Organisation, Neuilly-sur-Seine